Molecular Therapy
Oncolytics
Original Article

Inhibition of MEK-ERK pathway enhances oncolytic vaccinia virus replication in doxorubicin-resistant ovarian cancer

Seoyul Lee,[1] Wookyeom Yang,[1] Dae Kyoung Kim,[1] Hojun Kim,[1] Minjoo Shin,[1] Kyung Un Choi,[2] Dong Soo Suh,[3] Yun Hak Kim,[4] Tae-Ho Hwang,[5] and Jae Ho Kim[1,6]

[1]Department of Physiology, School of Medicine, Pusan National University, Yangsan, Gyeongsangnam-do 50612, Republic of Korea; [2]Department of Pathology, Pusan National University Hospital, Busan 49241, Republic of Korea; [3]Department of Obstetrics and Gynecology, Pusan National University Hospital, Busan 49241, Republic of Korea; [4]Department of Anatomy and Department of Biomedical Informatics, School of Medicine, Pusan National University, Yangsan, Gyeongsangnam-do 50612, Republic of Korea; [5]Gene and Cell Therapy Research Center for Vessel-associated Diseases, School of Medicine, Pusan National University, Yangsan, Gyeongsangnam-do 50612, Republic of Korea; [6]Biomedical Research Institute, Pusan National University Yangsan Hospital, Yangsan, Gyeongsangnam-do 50612, Republic of Korea

Oncolytic vaccinia virus (OVV) has been reported to induce cell death in various types of cancer; however, the oncolytic activity of OVV in drug-resistant ovarian cancer remains limited. In the present study, we established doxorubicin-resistant ovarian cancer cells (A2780-R) from the A2780 human ovarian cancer cell line. Both A2780 and A2780-R cells were infected with OVV to explore its anticancer effects. Interestingly, OVV-infected A2780-R cells showed reduced viral replication and cell death compared with A2780 cells, suggesting their resistance against OVV-induced oncolysis; to understand the mechanism underlying this resistance, we explored the involvement of protein kinases. Among protein kinase inhibitors, PD0325901, an MEK inhibitor, significantly augmented OVV replication and cell death in A2780-R cells. PD0325901 treatment increased the phosphorylation of STAT3 in A2780-R cells. Moreover, cryptotanshinone, a STAT3 inhibitor, abrogated PD0325901-stimulated OVV replication. Furthermore, trametinib, a clinically approved MEK inhibitor, increased OVV replication in A2780-R cells. Transcriptomic analysis showed that the MEK inhibitor promoted OVV replication via increasing STAT3 activation and downregulating the cytosolic DNA-sensing pathway. Combined treatment with OVV and trametinib attenuated A2780-R xenograft tumor growth. These results suggest that pharmacological inhibition of MEK reinforces the oncolytic efficacy of OVV in drug-resistant ovarian cancer.

INTRODUCTION

Ovarian cancer is one of the most common gynecological cancers and has the highest mortality rate.[1] Most patients with ovarian cancer (70%–80%) are diagnosed at an advanced stage, and they experience frequent relapse despite appropriate treatment alternatives such as surgical debulking and first-line chemotherapy based on platinum and taxanes.[2] Doxorubicin, a potent topoisomerase II inhibitor,[3] exhibits anti-tumor effects by inducing DNA damage through DNA intercalation, reactive oxygen species generation by redox cycling of the quinone structure, and suppressing DNA synthesis through topoisomerase II inhibition.[4] However, 50% of patients with ovarian cancer experience relapse within 12 months after front-line chemotherapy, and one-quarter of all relapses are incurred within 6 months,[5] attributable to acquired drug resistance.[6] Recurrent ovarian cancer originates from drug-resistant cancer cells that can develop by intrinsic or acquired causes via tumor heterogeneity after chemotherapy.[7] Most drug-resistant cancer cells have multidrug resistance and can tolerate the extremely severe tumor microenvironment. Drug-resistant ovarian cancer is more aggressive toward cancer treatment, and such patients experience poor prognosis after recurrence. Therefore, patients with recurrent ovarian cancer need more effective and efficient treatment methods than conventional therapy.

Oncolytic vaccinia virus (OVV) has been developed to selectively induce cancer cell death, and its safety has been demonstrated in various clinical trials.[8,9] There are several clinical benefits of OVV in cancer therapy. First, OVV has a large viral genome that allows it to tolerate large foreign DNA fragments[10]; second, the whole life cycle of OVV occurs in the cytoplasm of the host, thus preventing integration of the viral genome to the host genome[11]; and third, viral thymidine kinase (TK)-deleted OVV shows attenuated replication in normal cells.[12] Viral TK differs structurally and biologically from the mammalian host enzyme; it plays a critical role in synthesizing DNA and maintaining a high nucleotide pool.[13] The wild-type vaccinia virus has the TK gene induce cytoplasmic nucleotide pool in normal host cells, and they can rapidly replicate and induce damage of

Received 24 August 2021; accepted 15 April 2022;
https://doi.org/10.1016/j.omto.2022.04.006.

Correspondence: Department of Physiology, School of Medicine, Pusan National University, Yangsan, Gyeongsangnam-do 50612, Republic of Korea.
E-mail: jhkimst@pusan.ac.kr

normal host cells. However, TK-deleted OVV cannot replicate efficiently in normal cells, having insufficient nucleotide pool to activate the viral factory for replication. However, TK-depleted OVV actively replicates in cancer cells due to sufficient cytoplasmic nucleotide pool, leading to cell death,[12] presenting tumor selectivity of OVV. Therefore, the application of OVV in cancer therapy has many advantages.

Accumulating evidence suggests that OVV combined with chemotherapy or immunotherapy showed better clinical outcomes.[14] OVV has been reported to inhibit the growth of tumor cells with multiple drug-resistant phenotypes *in vivo* and *in vitro*.[15] Combined therapeutic strategies with OVV and various drugs, such as alkylating agents,[16] immune checkpoint inhibitors,[17] and protein kinase inhibitors,[18] have been shown to enhance the oncolysis efficacy against tumor cells and circumvent tumor resistance mechanisms.[19] Furthermore, OVV-based virotherapy could be enhanced by combining with rapamycin, cyclophosphamide, or gemcitabine.[20,21] GLV-1h68 effectively killed sorafenib-resistant hepatocellular carcinoma cells.[22] However, in a phase IIb clinical trial, OVV-based virotherapy using Pexa-Vec did not improve overall survival of patients with hepatocellular carcinoma when used as second-line therapy following sorafenib failure.[23] Therefore, it is still unclear whether OVV monotherapy can eradicate drug-resistant cancer cells or if it is necessary to develop combination therapy of OVV to enhance its therapeutic effect in drug-resistant ovarian cancer.

Therefore, this study aimed to evaluate the anticancer effects of OVV in doxorubicin-resistant ovarian cancer. We observed that inhibition of the mitogen-activated protein kinase (MEK-ERK) signaling promoted replication and cytotoxicity of OVV in doxorubicin-resistant cancer cells. Combining OVV virotherapy with an MEK inhibitor can improve the therapeutic efficacy of OVV in patients with ovarian cancer.

RESULTS

Establishment of drug-resistant cells from A2780 ovarian cancer cells

To mimic drug-resistant cancer cells of patients with recurrent ovarian cancer *in vitro,* we generated drug-resistant ovarian cancer cells (A2780-R) by continuous treatment of the A2780 human ovarian cancer cell line with doxorubicin. During repeated passaging, A2780-R cells showed distinct morphology from their parent cells (Figure 1A). A previous report suggested that recurrent cancer cells acquire stem-like characteristics along with drug resistance.[24] Therefore, we determined the expression levels of aldehyde dehydrogenase 1 (ALDH1) and multidrug-resistant ABC transporters (ABCB1 and ABCG2), which have been reported as cancer stem cell-related markers.[25,26] The protein levels of ALDH1, ABCB1, and ABCG2 were significantly upregulated in A2780-R cells compared with those in A2780 cells (Figure 1B). Consistently, the enzyme activity of ALDH was greater in A2780-R cells than that in A2780 cells (Figure 1C). Moreover, the expression of cancer stem cell markers, CD44 and SOX2, in A2780-R cells was greater than that in A2780 cells (Figure S1). In addition, we found that A2780-R cells were more resistant to doxorubicin and cisplatin than their parental cells (Figure 1D). These results indicated successful preparation of drug-resistant cells from the A2780 ovarian cancer cell line *in vitro*.

OVV replication attenuation in A2780-R cells compared with A2780 cells

OVV is a recombinant vaccinia virus that was formed by deletion of the TK gene and insertion of the GFP gene into the TK locus of the wild-type vaccinia virus (Figure 2A). Consequently, OVV-infected cells expressed GFP *in vitro*. OVV has been reported to induce cell death in drug-resistant cancer cells.[27] To evaluate the oncolytic effect of OVV in the drug-resistant ovarian cancer model, we infected ovarian cancer cells with OVV at 0.01 MOI and acquired green fluorescence images at the indicated time points (Figure 2B). Contrary to expectations that OVV would infect cancer cells regardless of being drug resistant, viral replication was significantly reduced in A2780-R cells. The flow cytometric analysis indicated significantly reduced viral replication and cell death by OVV infection in A2780-R cells compared with equally infected A2780 cells (Figures 2C and 2D). Measurement of viral titers using 10-fold serial dilutions of OVV exhibited reduced OVV expression in A2780-R cells compared with A2780 cells (Figure S2). To confirm these results, we established another doxorubicin-resistant ovarian cancer cell line (OVCAR3-R) from OVCAR3 cells, and the OVCAR3-R cells exhibited reduced OVV replication than their parental OVCAR3 cells (Figure S3). These results indicated that drug-resistant cancer cells attenuated viral replication compared with drug-sensitive cancer cells.

Increase in viral replication and OVV-mediated cell death by MEK inhibitor

For the enhanced oncolytic virotherapy of ovarian cancer, it is essential to abolish the reduced OVV replication of drug-resistant cancer cells. Previous reports suggested a crucial role of AMP-activated protein kinase (AMPK),[28] AKT,[29,30] and ERK[31] in viral replication and life cycle, as well as cancer malignancy.[32] MEK signaling has been reported to regulate viral replication.[33,34] Therefore, we examined the phosphorylation levels of protein kinases in A2780 and A2780-R cells. The phosphorylation levels of AKT and ERK proteins were observed to be significantly reduced in A2780-R cells (Figure 3A). To explore the role of the protein kinases on OVV replication, the effects of AMPK, AKT, or MEK inhibitors on OVV replication in A2780 and A2780-R cells were investigated. Interestingly, the AMPK inhibitor Compound C and the MEK inhibitor PD0325901 significantly increased OVV replication in A2780-R cells with more potent increase by PD0325901 (Figure 3B). To determine the optimal concentration of PD0325901, A2780-R cells were treated with increasing doses of PD0325901, and OVV infection and cell death were analyzed by flow cytometry. PD0325901 treatment dose-dependently increased the OVV infection and cell death in A2780-R cells (Figures 3C and 3D). Since PD0325901 treatment maximally increased cell death of A2780-R

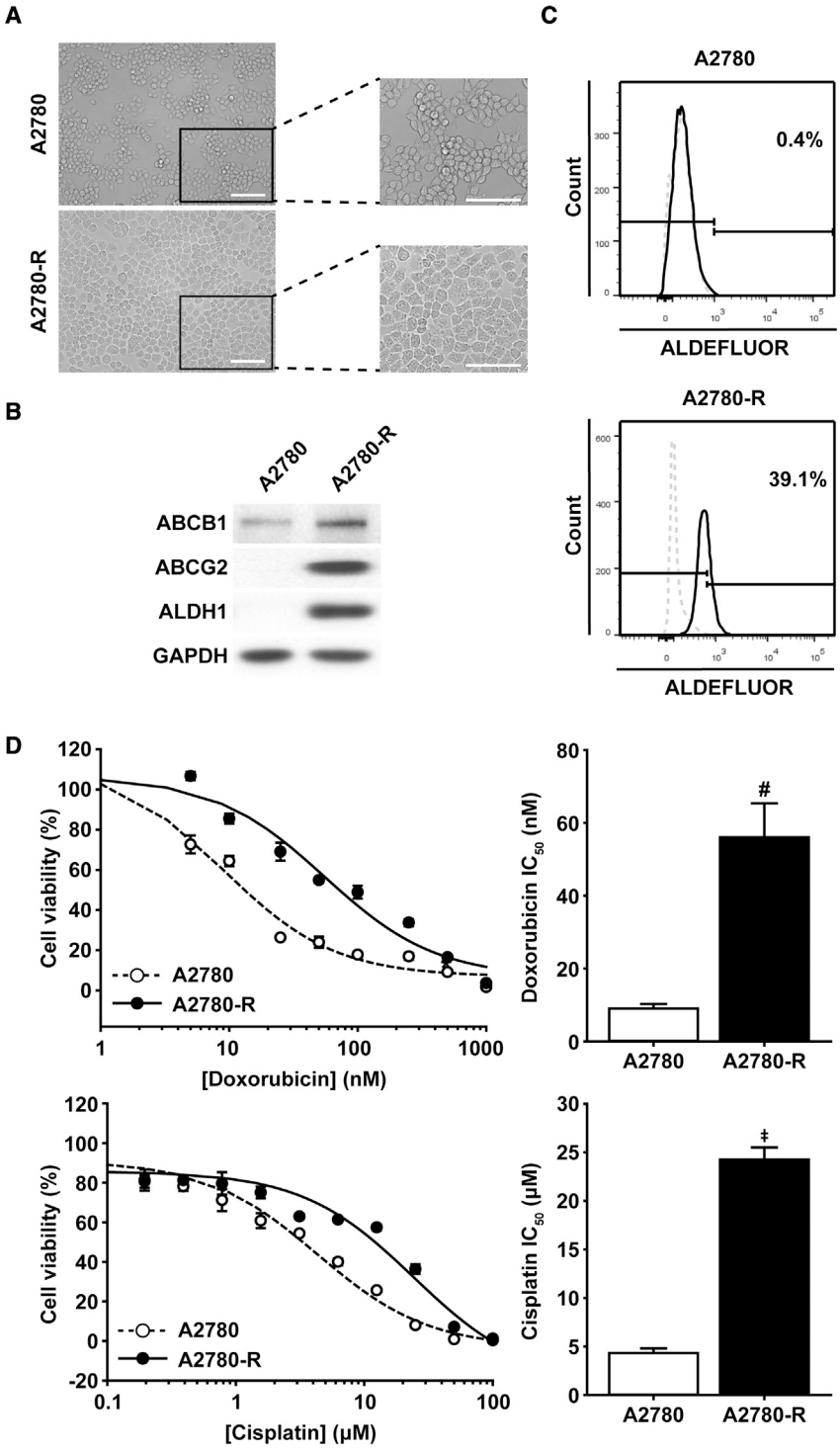

Figure 1. Generation of drug-resistant ovarian cancer cells from A2780 human ovarian cancer cell line

(A) Bright-field images of A2780 cells and A2780-R cells. Scale bar, 200 μm. (B) The expression of indicated proteins in A2780 and A2780-R cell lysates as measured by western blot analysis. GAPDH was used as a loading control. (C) Flow cytometric analysis for measuring the ALDH enzymatic activity in A2780 and A2780-R cells. (D) Cell viability as determined by the MTT assay. A2780 and A2780-R cells were treated with doxorubicin or cisplatin at indicated concentrations for 48 h. Data are represented as mean ± SEM. $^{*}p < 0.05$; $^{\#}p < 0.01$; $^{\ddagger}p < 0.001$.

cells at 2 μM concentration, 2 μM PD0325901 was used at subsequent experiments. Fluorescence imaging confirmed that PD0325901 treatment stimulated OVV-mediated GFP expression in both A2780 and A2780-R cells with more potent increase of OVV-derived GFP expression in A2780-R cells (Figure 3E). Moreover, the viral titer of OVV in A2780-R cells was more greatly enhanced by PD0325901 treatment than that in A2780 cells (Figure S4). These results suggest that MEK signaling pathways negatively regulate OVV replication in cancer cells.

Phosphorylation of STAT3 through MEK inhibition promotes OVV replication in drug-resistant A2780-R cells

To elucidate the molecular mechanism associated with PD0325901-stimulated viral replication, we compared the effects of PD0325901 on cell signaling in A2780 and A2780-R cells. The basal ERK phosphorylation level was greatly reduced in A2780-R cells compared with A2780 cells, and PD0325901 treatment further attenuated the ERK phosphorylation levels (Figure 4A). It has been previously reported that STAT3 plays a key role in vaccinia virus replication by promoting energy metabolism.[35] In contrast to ERK phosphorylation, the basal STAT3 phosphorylation level was higher in A2780-R cells than in A2780 cells, and PD0325901 treatment further increased STAT3 phosphorylation in A2780-R cells (Figure 4A, right panel). To investigate whether STAT3 is involved in PD0325901-stimulated OVV replication, we examined the effects of cryptotanshinone, a STAT3 inhibitor, on OVV replication. Cryptotanshinone treatment completely abrogated PD0325901-stimulated OVV replication in A2780-R cells (Figures 4B and 4C). Moreover, the basal and PD0325901-stimulated GFP expression in A2780 cells was also attenuated by cryptotanshinone treatment. Consistently, PD0325901-stimulated oncolytic cell death of both A2780 and A2780-R cells was abolished by cryptotanshinone treatment (Figure 4D). These results suggest that STAT3 activation plays a pivotal role in MEK inhibitor-stimulated OVV replication and virotherapy.

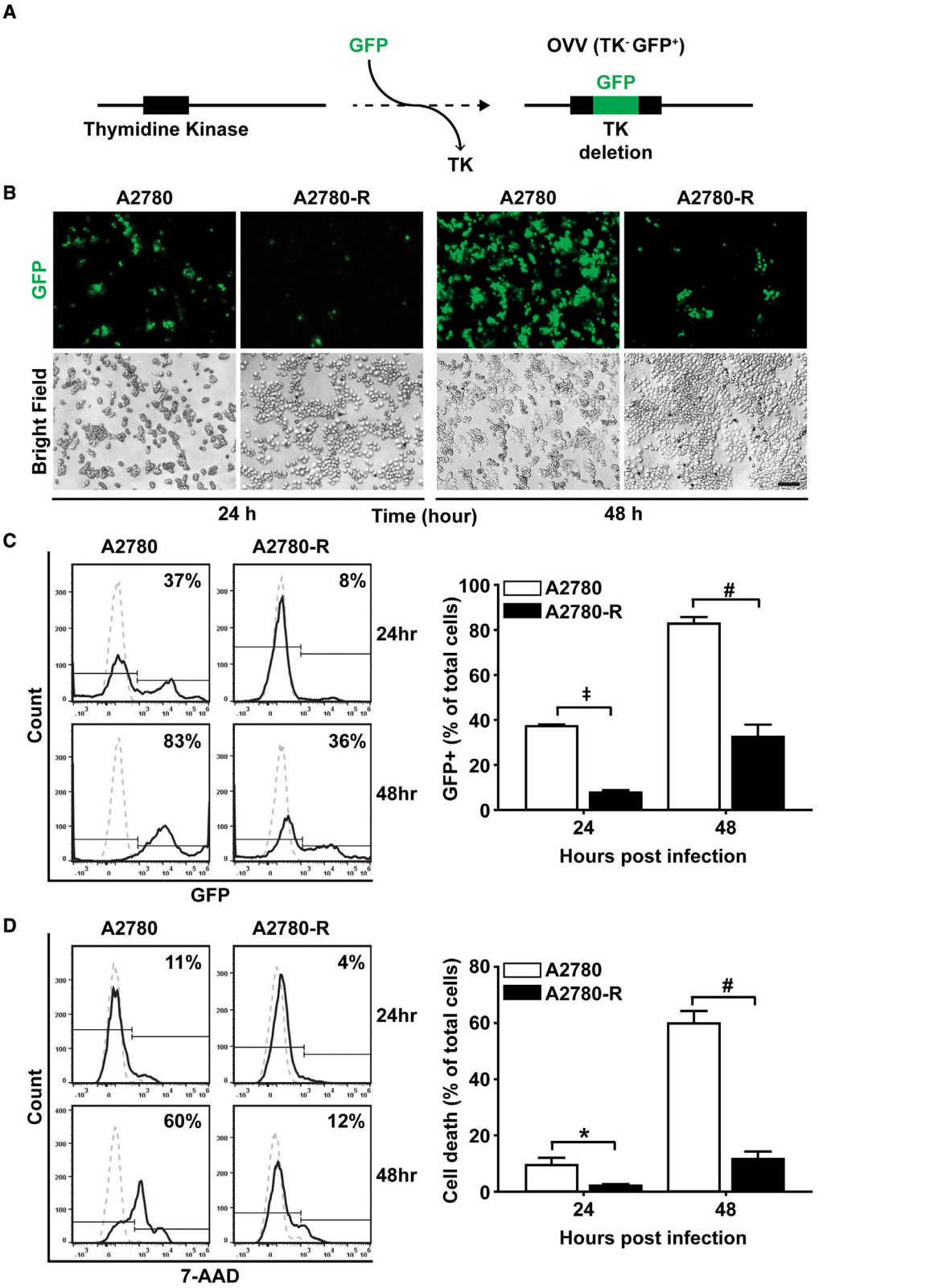

(legend on next page)

Trametinib, a Food and Drug Administration-approved MEK inhibitor, enhances the oncolytic effect of OVV

Several Food and Drug Administration (FDA)-approved MEK inhibitors, including trametinib, cobimetinib, binimetinib, selumetinib, and cobimetinib, have been developed for treatment of patients with melanoma, non-small cell lung cancer, and thyroid cancer.[36] To examine the effects of the FDA-approved MEK inhibitors on OVV-based virotherapy, we examined the effects of cobimetinib, trametinib, and sorafenib on OVV replication in A2780 and A2780-R cells. Both trametinib and cobimetinib significantly increased the OVV-mediated GFP expression in A2780 and A2780-R cells (Figure 5A). However, sorafenib exhibited no significant effect on OVV-mediated GFP expression in either cell type. Since the effect of trametinib on OVV-mediated GFP expression was more potent than that of cobimetinib, trametinib was used in the following experiments as an FDA-approved drug. Consistent with the A2780-R results, OVV replication in OVCAR3-R cells was also enhanced by trametinib treatment (Figure S5). To confirm whether trametinib-induced increased OVV replication was associated with STAT3 signaling, OVV-infected A2780 cells were treated with trametinib and cryptotanshinone. The OVV-derived GFP expression was increased after trametinib treatment, but completely abrogated by cryptotanshinone treatment in both A2780 and A2780-R cells (Figures 5B and 5C). In addition, trametinib treatment abrogated ERK phosphorylation but increased STAT3 phosphorylation levels, and cryptotanshinone treatment abolished the trametinib-stimulated STAT3 phosphorylation in A2780-R cells (Figure 5D). These results suggest that trametinib treatment promotes OVV replication and cell death through a STAT3-dependent mechanism in drug-resistant ovarian cancer cells.

MEK inhibition in A2780-R cells disturbs the expression of the cytoplasmic DNA-sensing genes

Since MEK inhibition in A2780-R cells accelerated the replication and oncolytic activity of OVV, we analyzed and compared the gene expression profiles in A2780-R cells treated with mock control or trametinib by mRNA sequencing (Figure 6A and Table S1). To elucidate the signaling pathways associated with MEK inhibition-stimulated OVV replication, we analyzed the genes through the Kyoto Encyclopedia of Genes and Genomes (KEGG) database (Table S1).[37] We found that the expression of genes involved in the cytosolic DNA-sensing pathway (Entry: map04623), including interferon regulatory factor 3 (*IRF3*) and DNA-directed RNA polymerase III subunits C, D, E, and K (*POLR3C, D, E, K*), were significantly downregulated in the trametinib-treated group (Figures 6B and S6). These results suggest that MEK inhibition enhances OVV replication in A2780-R cells by abrogating cytosolic DNA sensing and viral defense (Figure 6C).

Trametinib stimulates OVV-based virotherapy in the drug-resistant ovarian cancer xenograft model

To investigate whether trametinib stimulates OVV-based virotherapy *in vivo*, A2780-R cells were subcutaneously transplanted into nude mice, followed by combined treatment with OVV and trametinib (Figure 7A). OVV was administered intratumorally once and trametinib was injected daily into the intraperitoneal cavity for 1 week, and the volume of tumor xenograft was measured for the subsequent 24 days. Only slight attenuation of the growth of xenograft tumors was observed by monotherapy with either trametinib or OVV. However, combined treatment of OVV with trametinib synergistically inhibited the tumor growth compared with the monotherapy (Figures 7B and 7C). Consistently, the tumor weight derived from the mice in the combination group was the lowest among all groups (Figure 7D). Furthermore, we measured survival of A2780 and A2780-R xenograft transplantation mice models. In the A2780-R-transplanted mouse model, the combination of trametinib and OVV significantly increased survival of mice compared with the mice treated with OVV alone (Figure S7). These results suggest that trametinib treatment can potentiate OVV-based virotherapy of drug-resistant ovarian cancer *in vivo*.

DISCUSSION

In the present study, we demonstrated that doxorubicin-resistant A2780-R cells exhibited resistance against OVV therapy and showed reduced OVV replication. We showed that the combination of OVV and MEK inhibition augmented death of A2780-R cells through increased viral replication *in vitro*. In addition, tumor growth was attenuated by combined treatment with OVV and the FDA-approved MEK inhibitor, trametinib, in an *in vivo* xenograft mouse model. Previous studies have reported that the activity of EGF receptor-Ras-Raf-MEK-ERK signaling is essential for OVV replication.[33,34] The inhibition of MEK signaling has been negatively or positively correlated with viral replication depending on the types of oncolytic viruses and cells. It has been previously reported that MEK inhibition suppressed vaccinia virus replication in human fibroblasts without affecting cell viability.[35] However, it has been reported that MEK inhibition increased cancer cell apoptosis via enhancing oncolytic viral replication and melanoma-specific adaptive immune responses.[38] MEK inhibition also enhanced oncolytic adenovirus replication and tumor cell death through upregulation of the coxsackievirus and adenovirus receptor.[39] On the contrary, viral replication-independent mechanisms underlying MEK inhibitor-stimulated virotherapy have also been reported. The combination treatment with oncolytic reovirus and the MEK inhibitor PD184352 increased cancer cell death due to endoplasmic reticulum stress-induced apoptosis regardless of viral replication.[40] The replication-competent oncolytic herpes simplex mutant virus NV1066 played as a sensitizing agent for

Figure 2. Increased resistance of A2780-R cells against oncolytic vaccinia virus

(A) The schematic diagram of the TK-GFP + OVV, which is a TK gene-inactivated OVV expressing GFP instead of TK gene. (B) Green fluorescence (upper) and bright-field (lower) images of A2780 and A2780-R cells after infection with OVV (MOI = 0.01) at indicated time points. Scale bar, 200 μm. (C and D) Flow cytometric analysis of OVV-mediated GFP expression and oncolytic cell death in A2780 and A2780-R cells. The relative percentage was indicated as GFP-positive cells (OVV-infected cells) (C) and dead cells (D). Data are represented as mean ± SEM. $^{*}p < .05$; $^{\#}p < 0.01$; $^{\ddagger}p < 0.001$.

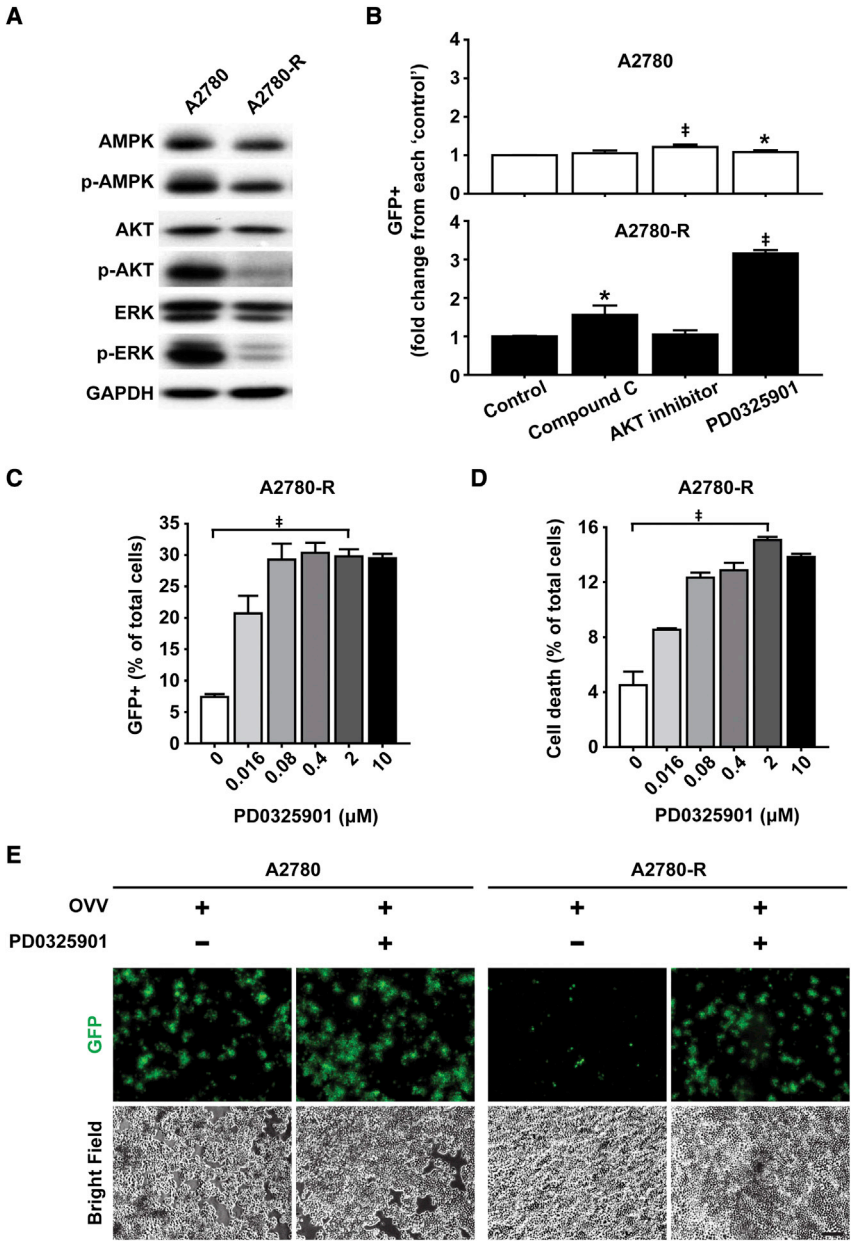

Figure 3. Effects of the MEK inhibitor on OVV replication and oncolytic cell death in A2780 and A2780-R cells

(A) The expression and phosphorylation levels of AMPK, AKT, and ERK in A2780 and A2780-R cells were measured by western blot analysis. GAPDH was used as a loading control. (B) Flow cytometric analysis of GFP expression in A2780 and A2780-R cells. The cells were pre-treated with the indicated inhibitors (10 μM Compound C, 10 μM AKT inhibitor, 10 μM PD0325901), followed by OVV infection (0.01 MOI) for 24 h. The GFP expression levels were determined by flow cytometric analysis and normalized to the respective control group. (C and D) Dose-dependent effect of PD0325901 on OVV-mediated GFP expression and oncolytic cell death in A2780-R cells. In flow cytometric analysis of A2780-R cells, cells were treated with increasing doses of PD0325901 in combination with OVV infection (0.01 MOI). These graphs indicate the relative percentage of GFP-positive cells (C) and dead cells (D). (E) Green fluorescence (upper) and bright-field (lower) images of A2780 and A2780-R cells after OVV infection (0.01 MOI) in the absence or presence of 2 μM PD0325901. Scale bar, 200 μm. Data are represented as mean ± SEM. *$p < 0.05$; #$p < 0.01$; ‡$p < 0.001$.

conventional chemotherapy by downregulating the MEK/ERK pathway in triple-negative breast cancer.[41] MEK inhibitor PD98059 reduced autophagy and increased glioma cell death without elevating oncolytic adenovirus replication.[42] Therefore, it is likely that MEK inhibition affects oncolytic virotherapy depending on the types of oncolytic virus.

Trametinib is a type III allosteric, non-competitive, and highly selective MEK1/2 inhibitor. Trametinib has been reported to inhibit RAF-induced MEK activity and ERK phosphorylation,[43] and it has been approved by the FDA to treat several cancers with BRAF V600E mutation, including metastatic non-small cell lung cancer, metastatic melanoma, and advanced or metastatic anaplastic thyroid cancer.[44–46] Several reports suggested that the potential mechanism of MEK1/2 pathway inhibition by trametinib is highly effective for the treatment of high-grade serous ovarian carcinoma, KRAS-mutated ovarian cancer, and platinum-Taxol-resistant ovarian cancer.[47–49] We demonstrated, for the first time, that the combination therapy with OVV and trametinib synergistically eradicated OVV/drug-resistant ovarian cancer *in vitro* and *in vivo*. Although trametinib has not yet been approved for use in patients with ovarian cancer, it will be interesting to explore whether the combination therapy of OVV with trametinib or cobimetinib can be applied in clinical trials for improved therapeutic efficacy.

The present study demonstrated that MEK inhibition led to increased STAT3 activation in A2780 cells. A2780-R cells exhibited higher levels of phospho-STAT3 than parental A2780 cells, and MEK inhibition further increased phospho-STAT3 levels, which were inversely correlated with phospho-ERK levels. Our results are consistent with previous studies reporting negative correlation between MEK/ERK signaling and STAT3 signaling in several cancer cells.[50–52] However, according to a previous study, the effects of STAT3 activity on viral replication are widely dependent on viral strain.[53] In this study, STAT3 inhibition abrogated the MEK inhibition-stimulated replication of OVV in A2780-R cells. Moreover,

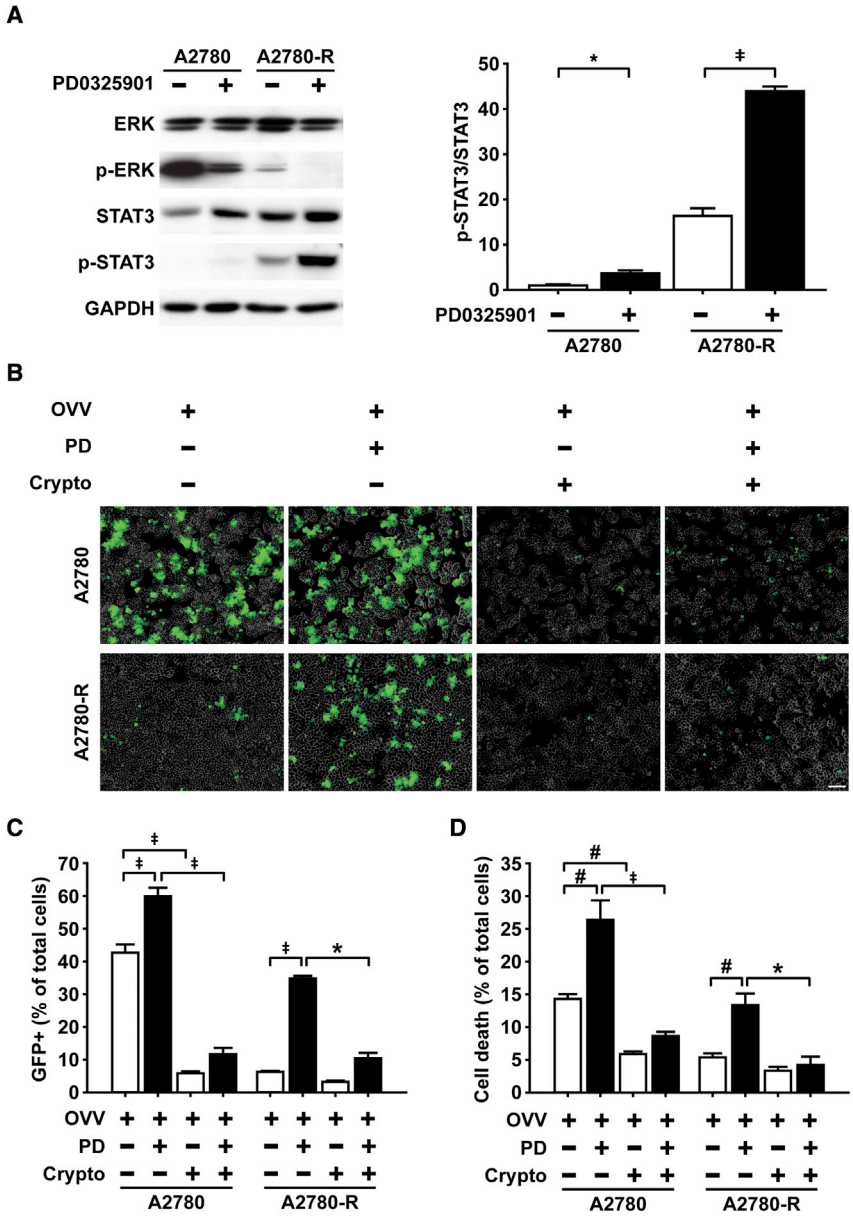

Figure 4. Role of STAT3 in the MEK inhibition-stimulated oncolytic cell death in A2780-R cells

(A) Effects of PD0325901 treatment on STAT3 activation in A2780-R cells. A2780 and A2780-R cells were treated with or without 2 μM PD0325901, and the expression and phosphorylation levels of ERK and STAT3 were determined by western blot analysis. GAPDH was used as a loading control. The right panel shows densitometric analysis of phospho-STAT3/total-STAT3 ratio of western blotting data. (B) A2780-R cells were treated with or without 2 μM PD0325901 or 10 μM cryptotanshinone for 24 h and then infected with 0.01 MOI OVV for 24 h. Scale bar, 100 μm. (C and D) Effects of the STAT3 inhibitor cryptotanshinone on PD0325901-stimulated OVV replication and oncolytic cell death. A2780 and A2780-R cells were treated with the indicated inhibitors along with OVV infection, followed by flow cytometric analysis. The relative percentages of GFP-positive cells (C) and dead cells (D) are shown. Data are represented as mean ± SEM. *$p < 0.05$; #$p < 0.01$; ‡$p < 0.001$. PD, PD0325901; Crypto, cryptotanshinone.

STAT3 activation has been reported to promote oncolytic herpes simplex virus replication in glioma cells.[54] STAT3 inhibitor has been identified to suppress vaccinia virus replication by screening compound library.[55] These results suggest that STAT3 activation is responsible for the increased OVV replication induced by MEK inhibition.

Many cancer cells have defects in the type I interferon (IFN) signaling pathway, which makes cancer cells more permissive to oncolytic virus replication.[56] Furthermore, IFN-α can antagonize oncolytic virus by suppressing replication and blocking virus-mediated apoptosis.[57] Treatment of cancer cells with inhibitors of IFN response, including the JAK1/2 inhibitor, ruxolitinib, and IFN-binding decoy receptors augmented oncolysis.[58] We found that the expression of genes associated with IFN signaling was significantly altered in A2780-R cells compared with their parental cells (Figure S8 and Table S2). Although the implication of IFN signaling in OVV resistance in A2780-R cells remains elusive, these results suggest that drug-resistant cancer cells can exhibit resistance against OVV therapy in addition to conventional anticancer drugs. Furthermore, we observed upregulation of STAT3 and downregulation of cytosolic DNA-sensing signaling in the trametinib-treated group. The whole life cycle of vaccinia virus, a double-stranded DNA virus, progresses in the host cytoplasm; consequently, activation of the cytosolic DNA-sensing pathway affects the host's vaccinia virus infection levels.[59] Consistently, reported study demonstrated that activation of STAT3 signaling promoted oncolytic herpes virus replication through inhibition of type I IFN signaling in glioma cells.[54] Therefore, these results suggest the novelty and potential of the combination therapy of OVV with MEK inhibitor in drug-resistant ovarian cancer.

The present study demonstrated that doxorubicin-resistant ovarian cancer cells were resistant to OVV-based virotherapy. Moreover, we demonstrated that the inhibition of MEK signaling in doxorubicin-resistant ovarian cancer cells promoted viral replication and OVV-mediated oncolytic effect via STAT3 activation. Clinical applications of these findings may result in eradication of drug-resistant ovarian cancer cells and serve as the basis of future studies on overcoming recurrent ovarian cancer.

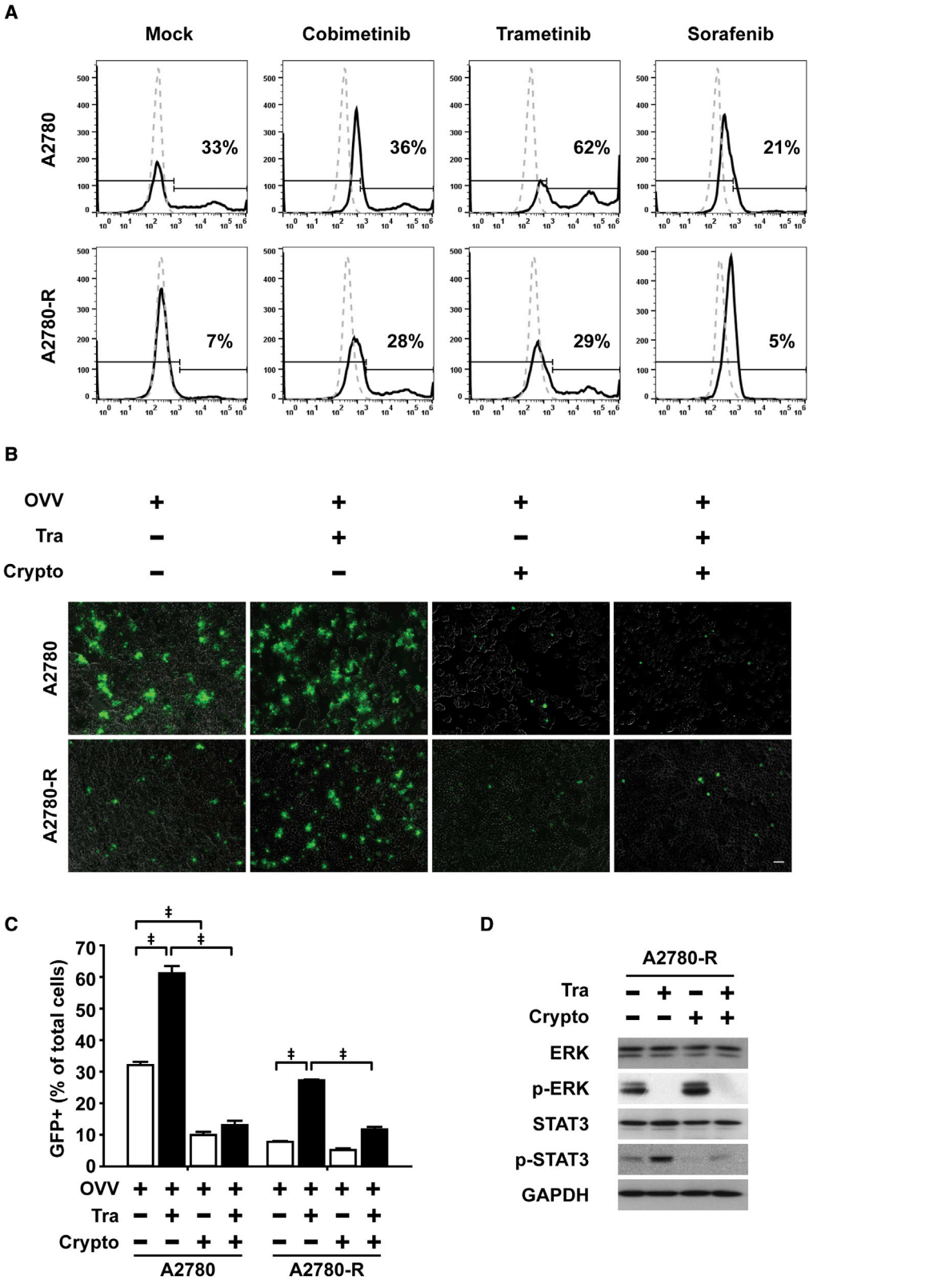

(legend on next page)

MATERIALS AND METHODS

Materials

RPMI1640 medium and trypsin-EDTA solution were purchased from Welgene (Gyeongsan, Gyeongsangbuk-do, Republic of Korea). Hank's balanced salt solution (HBSS), fetal bovine serum (FBS), penicillin-streptomycin solution, and cell culture plates for adherent cells were purchased from Thermo Fisher Scientific Inc. (Waltham, MA). Doxorubicin, 3-(4,5-dimethylthiazol-2-yl)-2,5-diphenyltetrazolium bromide (MTT), $Na_4P_2O_7 \cdot 10H_2O$, NaF, Na_3VO_4, EGTA, EDTA, Tris, NaCl, Triton X-100, PD0325901, and cryptotanshinone were purchased from Sigma-Aldrich (St. Louis, MO). AKT inhibitor and Compound C were obtained from Calbiochem (San Diego, CA). Trametinib was purchased from Cayman Chemical Company (Ann Arbor, MI). Cobimetinib and Sorafenib were purchased from ApexBio Technology (Houston, TX). The ALDEFLUOR Kit was purchased from STEMCELL Technologies (Vancouver, BC, Canada). TRIsure was purchased from Meridian Bioscience (Memphis, TN). HelixCript Thermo Reverse Transcriptase (with dNTP Mix) and HelixZyme RNase Inhibitor were purchased from NanoHelix (Yuseong-gu, Daejeon, Republic of Korea). Antibodies against glyceraldehyde-3-phosphate dehydrogenase (GAPDH) were purchased from Santa Cruz Biotechnology (Dallas, TX); 7-amino-actinomycin D (7-AAD) (#559925) and anti-aldehyde dehydrogenase (ALDH) (#611194) were purchased from BD Biosciences (Franklin Lakes, NJ). Antibodies against ABCG2 (ab3380) and SOX2 (ab97959) were purchased from Abcam (Cambridge, UK). Antibodies against AMPK (#5832), p-AMPK (#2535), AKT(#9272), p-AKT (#9271), CD44 (#5640), ERK (#9102), p-ERK (#9101), STAT3 (#9139), and p-STAT3 (#9131) were purchased from Cell Signaling Technology (Danvers, MA).

Cell lines and virus

A2780 and OVCAR3, the human ovarian cancer cell lines, were cultured in RPMI1640 medium supplemented with 10% FBS and penicillin-streptomycin solution (100 units/mL and 100 μg/mL, respectively). Doxorubicin-resistant A2780 (A2780-R) and OVCAR3 (OVCAR3-R) cells were established from A2780 or OVCAR3 by repeated subculturing in the presence of doxorubicin. To increase resistance against doxorubicin of these cells, we repeatedly doubled supplementing doxorubicin concentration from 1 nM up to 128 nM. U2OS was cultured in DMEM supplemented with 10% FBS and penicillin-streptomycin solution.

OVV was a western reserve strain and had a TK-deleted genotype by inserting the GFP gene into the TK locus.[60]

OVV infection

Cells (2×10^5/well) were seeded in 24-well plates 24 h before treatment with or without the indicated inhibitor. After 24 h, each cell line was infected with OVV at indicated MOI. After 24 to 48 h, 24-well plates were imaged under phase-contrast (bright field) or fluorescence microscopy using the EVOS M5000 Imaging System (Thermo Fisher Scientific) or were analyzed by flow cytometry.

Western blotting

Cells were washed twice with HBSS and lysed using lysis buffer (30 mM $Na_4P_2O_7 \cdot 10H_2O$, 20 mM NaF, 1 mM Na_3VO_4, 1 mM EGTA, 1 mM EDTA, 20 mM Tris-HCl, 10 mM NaCl, and 1% Triton X-100; pH 7.4). The cell lysates were centrifuged for 15 min at 4°C, and the supernatants were used for western blotting. The protein samples were separated by SDS-PAGE, transferred onto nitrocellulose membranes, and then stained with 0.1% Ponceau S solution (Sigma-Aldrich) to ensure equal loading of the samples. After blocking with 5% non-fat milk for 30 min, the membranes were incubated with the primary antibodies overnight, and the bound antibodies were visualized with horseradish peroxidase-conjugated secondary antibodies using an enhanced chemiluminescence western blotting system (Amersham Biosciences, Piscataway, NJ).

Flow cytometry analysis

ALDH activity was detected using the ALDEFLUOR Kit, as described by the manufacturer. Analysis of the fluorescence intensity of the stained cells was performed using CANTO II (BD Biosciences). The ALDH activity of the cells was determined based on fluorescence intensity beyond the threshold as defined by the reaction with diethylaminobenzaldehyde. GFP fluorescence and cell death assays were performed after OVV infection, as described above. Following infection for 24 to 48 h, cells were washed with HBSS twice and detached using trypsin-EDTA solution. Then, the cells were incubated in HBSS with or without 7-AAD for 10 min at 4°C. Cells labeled with virus-GFP or 7-AAD were analyzed using the Attune NxT Acoustic Focusing Cytometer (Thermo Fisher Scientific).

Cytotoxicity assay

To assess the viability of cells treated with doxorubicin, 5×10^3 cells were plated in 96-well plates in 100 μL growth medium supplemented with doxorubicin at the indicated concentration per well. After removal of the culture medium at different time points, the cells were washed twice with HBSS and incubated with 100 μL of MTT solution (0.5 mg/mL) for 2 h at 37°C. After incubation, formazan granules generated by the cells were dissolved in 100 μL of DMSO, and the

Figure 5. Effects of the FDA-approved MEK inhibitors on OVV replication and oncolytic cell death in A2780 and A2780-R cells

(A) A2780 and A2780-R cells were pre-treated with the cobimetinib, trametinib, or sorafenib, followed by OVV infection and flow cytometric analysis of GFP-positive population. The percentages of GFP-positive population are indicated. (B and C) Effect of the STAT3 inhibitor on the trametinib-stimulated OVV replication. A2780 and A2780-R cells were pre-treated with 2 μM trametinib or 10 μM cryptotanshinone and then infected with 0.01 MOI OVV. After 24 h, GFP expression in A2780 and A2780-R cells was measured by fluorescence microscopy (B) and flow cytometric analysis (C). The scale in (B) indicates 100 μm. (D) Effects of the STAT3 inhibitor on the trametinib-stimulated STAT3 phosphorylation in A2780-R cells. The expression and phosphorylation levels of ERK and STAT3 were measured by western blotting. GAPDH was used as a loading control. Data are represented as mean ± SEM. $^*p < 0.05$; $^{\#}p < 0.01$; $^{\ddagger}p < 0.001$. Tra, trametinib; Crypto, cryptotanshinone.

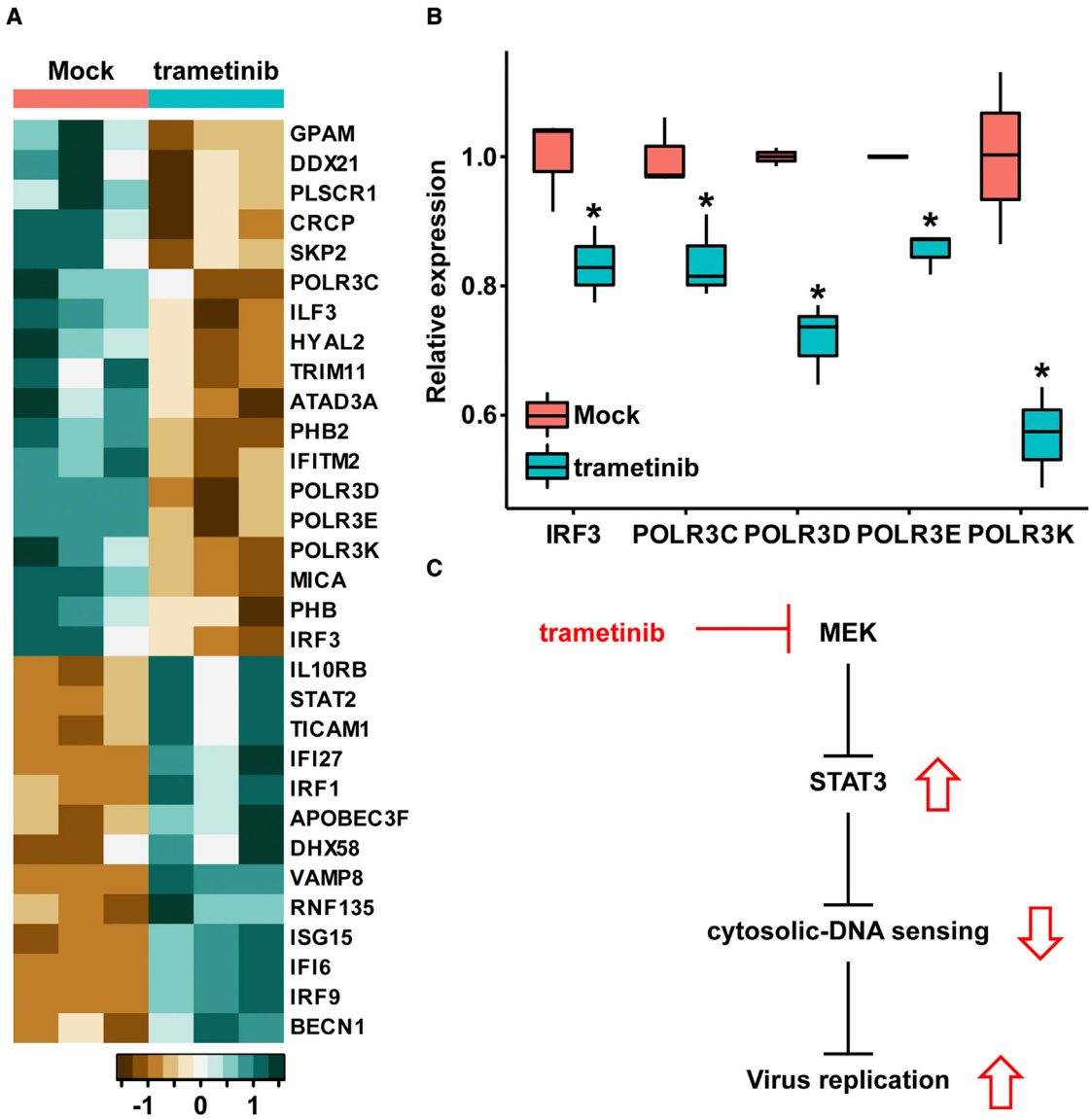

Figure 6. Effects of trametinib treatment on expression of the cytoplasmic DNA-sensing pathway-related genes in A2780-R cells

(A and B) The gene expression profiles of viral defense response were obtained from A2780-R treated with mock control or 2 μM trametinib for 24 h. (B) Relative TPM value of cytosolic DNA-sensing pathway-related genes among the virus defense genes. (C) A schematic diagram of cellular signaling for trametinib-treated A2780-R cells. See also Table S1. *p < 0.05.

absorbance of the solution at 570 nm was determined using the Sunrise Absorbance Reader (Tecan Trading AG, Switzerland).

Cell viability (%) and half maximal inhibitory concentration (IC_{50}) were calculated as follows.

$$\text{Cell viability}(\%) = \frac{\text{Exprimental group(Drug)absorbance}}{\text{Control group(Mock)absorbance}}$$

After calculating cell viability, we computed IC_{50} by conducting four-parameter logistic curve-fitting on each cell line. Furthermore, we compared IC_{50} values between wild-type and resistant cell lines using a t test.

Virus titration

We conducted a colorimetric-based tissue culture infective dose 50% ($TCID_{50}$) assay to measure viral titer.[61] First, we treated mock or 2 μM PD0325901 on A2780 and A2780-R cells for 24 h, and we infected OVV at 0.01 MOI to two cell lines for 24 h. After washing cells, we froze and heated cells three times using liquid nitrogen and a warmed water bath, and these lysates were sonicated and serially diluted by 5-fold after an initial 50-fold. We treated lysate to U2OS

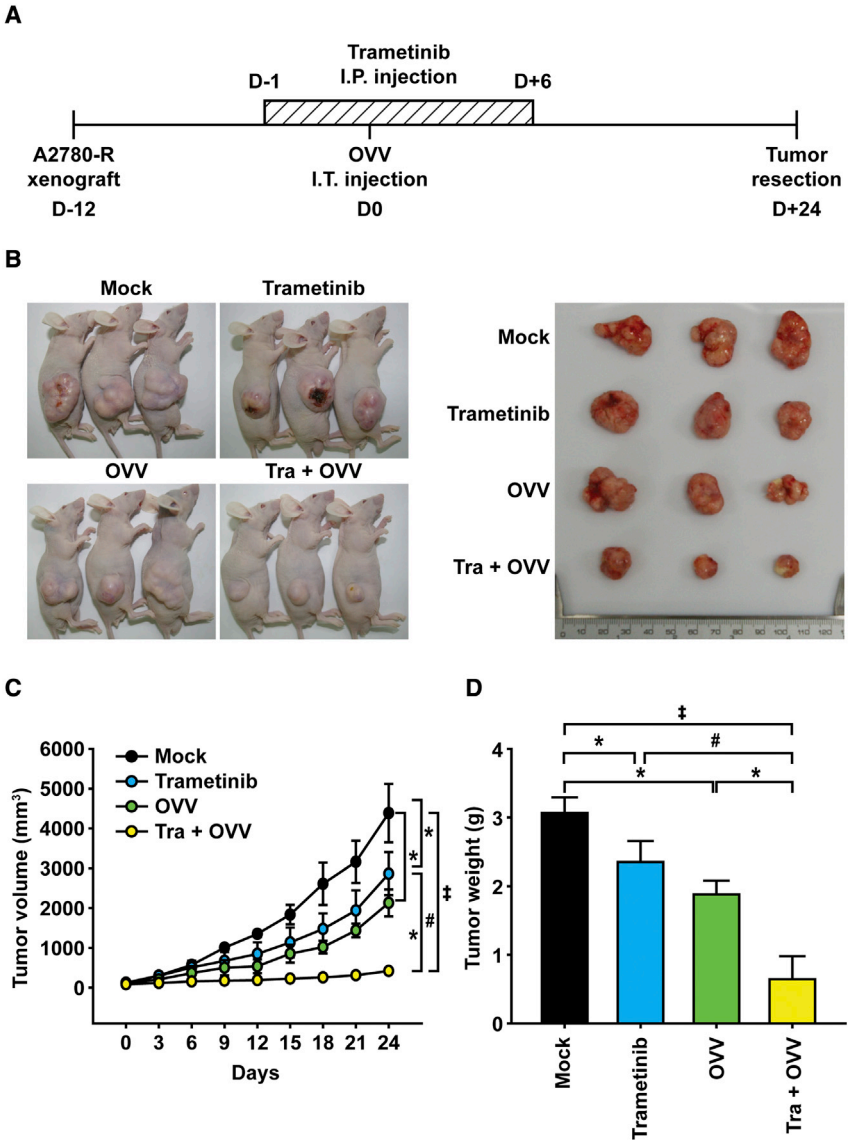

Figure 7. Combination therapy of OVV with trametinib diminishes tumor growth in the A2780-R cell-derived xenograft model

(A) BALB/c-nu/nu mice were subcutaneously transplanted with A2780-R cells on day −12, intraperitoneally injected vehicle (0.4% DMSO) or trametinib (0.5 mg/kg) daily from day −1 to day 6, and intratumorally injected with vaccinia virus (1×10^6 PFU) on day 0. (B) Representative images of the xenograft mice (left side) and tumor tissues (right side). (C) Effects of the combined treatment with trametinib and OVV on *in vivo* tumor growth of A2780-R cells. Tumor volume was determined from day 0 to day 24. (D) The tumor tissues were isolated from the xenograft mice on day 24 for measurement of the tumor weights. Data are represented as mean ± SEM. *$p < 0.05$; #$p < 0.01$; ‡$p < 0.001$.

cells for 72 h and calculated $TCID_{50}$ by MTT assay. Cytotoxicity (%) was calculated as "100%-cell viability value," and $TCID_{50}$ was calculated with the same method as IC_{50} using cytotoxicity value. $TCID_{50}$/mL value was calculated as $TCID_{50} \times$(1 mL/treated volume).

Transcriptome sequencing and gene expression profile analysis

A2780 and A2780-R cells were treated with mock control or 2 μM trametinib for 24 h. For library construction, RNA extraction was performed with TRIsure reagent according to the product manual. After quality control, qualified samples were used for library construction. The sequencing library was prepared by random fragmentation of the sample, followed by 5′ and 3′ adapter ligation. Adapter-ligated fragments were then amplified using PCR and purified using gel extraction. The library was loaded into a flow cell for cluster generation, where fragments were captured on a lawn of surface-bound oligos complementary to the library adapters. Each fragment was then amplified into distinct clonal clusters by bridge amplification. When cluster generation was complete, the templates were sequenced on Illumina NovaSeq 6000 that generates raw images using sequencing control software for system control and base calling through an integrated primary analysis software called the Real Time Analysis. The binary base call (BCL) files were converted into FASTQ by using the Illumina package bcl2fastq.

The raw reads obtained through sequencing were preceded by quality control analysis. It produced basic statistics such as overall read quality, total bases, total reads, and guanine-cytosine (GC) content (%). In order to reduce the bias of the analysis result, it has low quality or goes through pre-processing, which removes artifacts such as adapter sequences, contaminant DNA, and PCR duplicates. For reads that had undergone preprocessing, we used the HISAT2 program that considers splice to map to the reference genome (hg19) and then generates aligned reads. Using the reference-based aligned read information, transcript assembly was performed through the StringTie program. The expression level obtained through transcript quantification of each sample was calculated as Fragments Per Kilobase of transcript per Million mapped reads (FPKM) value or Transcripts Per Million (TPM) value, and the expression profile was extracted using these normalized values.

To analyze the gene expression profile of the virus response, we used the gene ontology (GO) term "defense response to virus" (accession GO:0051607).[62] Total annotations in this GO term were filtered by organism *Homo sapiens*. Among the filtered genes, a heatmap was generated with the genes that showed statistical significance between the mock control and the trametinib group. Gene set enrichment

Primer list

	Sequence (5′->3′)
IRF3-Forward	TCTGCCCTCAACCGCAAAGAAG
IRF3-Reverse	TACTGCCTCCACCATTGGTGTC
POLR3C-Forward	ATTGCCCATGACACAGGAAC
POLR3C-Reverse	ACACCACGTTTGTGCACTTG
POLR3D-Forward	TCGGGGGAGTCAAGAAGAAAAC
POLR3D-Reverse	TCTGTCCCTTTCACGCTTCTC
POLR3E-Forward	TCCACCTGACACCTTTACATGG
POLR3E-Reverse	TAACATCGTCTTCCGCCTCATC
POLR3K-Forward	TGCCTGGGAGAATGTTGACTC
POLR3K-Reverse	ACTGAGCATTGCAGCACTTG
C1S-Forward	TGACCTTGCGGAGAGAAGAT
C1S-Reverse	TGTAGCGGATGACAGAACCA
PROCR-Forward	CCTTTCCTCTGACCATCC
PROCR-Reverse	GCAGTTCATACCGAGTGC

analysis was performed with the Hallmark Gene Sets database using the GSEA software (4.1.0).

Quantitative RT-PCR

Sample preparation process was the same as the above transcriptome sequencing. After RNA extraction, reverse transcription was performed using the HelixCript Thermo Reverse Transcriptase (with dNTP Mix) product and RNase inhibitor according to the product manual. Quantitative PCR was conducted by ABI7500 (Applied Biosystems, Foster City, CA) using SYBR Green PCR Master Mix according to the manufacturer's manual.

In vivo xenograft tumor transplantation model

All animal studies were conducted according to the protocols approved by the Pusan National University Institutional Animal Care and Use Committee (PNU-2018-1816). A2780-R cells (1×10^5) were suspended in 100 μL of 50% Matrigel solution (diluted with growth medium) and injected subcutaneously into the right flanks of 6- to 8-week-old BALB/c-nu/nu mice. We then observed the mice transplanted with tumor cells twice a week for the appearance of tumor. We measured the length (mm) and width (mm) of the tumor masses using a digital caliper and calculated the tumor volume (mm^3) as (length × $width^2$)/2 twice a week. We administered intraperitoneal injection containing vehicle (0.4% DMSO) or trametinib (0.5 mg/kg) daily from day 11 to day 18 and intratumoral injection containing sterile water or vaccinia virus (1×10^6 plaque-forming units [PFU]) on day 12. All mice were killed by anesthetic overdose on day 36.

For the survival experiment, the process of injecting cells (add A2780 cells) and monitoring the tumor is the same as above. After, we administered intraperitoneal injection containing vehicle (0.4% DMSO) or trametinib (0.5 mg/kg) daily from day 8 to day 14 and intratumoral injection containing sterile water or vaccinia virus (1×10^6 PFU) on day 9. All mice were euthanized when a tumor volume reached 2000 mm^3. Furthermore, we generated a Kaplan-Meier curve and executed a statistical test to compare survival among the experimental groups.

Statistical analysis

All statistical analyses were performed using the Prism 5 (GraphPad Software, San Diego, CA), SigmaPlot 10.0 (Systat Software, San Jose, CA), and R 4.1.0 (The R Foundation) packages: gplots and tidyverse. The data are presented as the mean ± SEM. Statistical significance was determined using two-tailed Student's t test or one-way ANOVA; $n \geq 3$, unless stated otherwise.

SUPPLEMENTAL INFORMATION

Supplemental information can be found online at https://doi.org/10.1016/j.omto.2022.04.006.

ACKNOWLEDGMENTS

We thank Dr. Eung-Kyun Kim (Pusan National University) for useful discussions. This research was supported by the MRC programs (NRF-2015R1A5A2009656) and research grants (NRF-2020R1I1A3073064; NRF-2020R1A2C2011880) of the National Research Foundation of Korea funded by the Ministry of Education, Science and Technology, Republic of Korea.

AUTHOR CONTRIBUTIONS

S.L. designed the study, performed experiments, analyzed data, and wrote the manuscript; W.Y., D.K.K., H. K., M. S., K.U.C., D.S.S., Y.H.K., and T.-H.H. performed experiments and analyzed data; J.H.K. supervised specific experiments and contributed to the study design and manuscript editing.

DECLARATION OF INTERESTS

The authors declare no competing interests.

REFERENCES

1. Bray, F., Ferlay, J., Soerjomataram, I., Siegel, R.L., Torre, L.A., and Jemal, A. (2018). Global cancer statistics 2018: GLOBOCAN estimates of incidence and mortality worldwide for 36 cancers in 185 countries. CA Cancer J. Clin. *68*, 394–424. https://doi.org/10.3322/caac.21492.

2. Pignata, S., Cecere, S.C., Du Bois, A., Harter, P., and Heitz, F. (2017). Treatment of recurrent ovarian cancer. Ann. Oncol. *28*, viii51–viii56. https://doi.org/10.1093/annonc/mdx441.

3. Pommier, Y., Leo, E., Zhang, H., and Marchand, C. (2010). DNA topoisomerases and their poisoning by anticancer and antibacterial drugs. Chem. Biol. *17*, 421–433. https://doi.org/10.1016/j.chembiol.2010.04.012.

4. Minotti, G., Menna, P., Salvatorelli, E., Cairo, G., and Gianni, L. (2004). Anthracyclines: molecular advances and pharmacologic developments in antitumor activity and cardiotoxicity. Pharmacol. Rev. *56*, 185–229. https://doi.org/10.1124/pr.56.2.6.

5. Ushijima, K. (2010). Treatment for recurrent ovarian cancer-at first relapse. J. Oncol. *2010*, 497429. https://doi.org/10.1155/2010/497429.

6. Oronsky, B., Ray, C.M., Spira, A.I., Trepel, J.B., Carter, C.A., and Cottrill, H.M. (2017). A brief review of the management of platinum-resistant-platinum-refractory ovarian cancer. Med. Oncol. *34*, 103. https://doi.org/10.1007/s12032-017-0960-z.

7. Vasan, N., Baselga, J., and Hyman, D.M. (2019). A view on drug resistance in cancer. Nature *575*, 299–309. https://doi.org/10.1038/s41586-019-1730-1.

8. Breitbach, C.J., Moon, A., Burke, J., Hwang, T.H., and Kirn, D.H. (2015). A phase 2, open-label, randomized study of pexa-vec (JX-594) administered by intratumoral injection in patients with unresectable primary hepatocellular carcinoma. Methods Mol. Biol. *1317*, 343–357. https://doi.org/10.1007/978-1-4939-2727-2_19.

9. Lauer, U.M., Schell, M., Beil, J., Berchtold, S., Koppenhofer, U., Glatzle, J., Konigsrainer, A., Mohle, R., Nann, D., Fend, F., et al. (2018). Phase I study of oncolytic vaccinia virus GL-ONC1 in patients with peritoneal carcinomatosis. Clin. Cancer Res. *24*, 4388–4398. https://doi.org/10.1158/1078-0432.CCR-18-0244.

10. Harrington, K., Freeman, D.J., Kelly, B., Harper, J., and Soria, J.C. (2019). Optimizing oncolytic virotherapy in cancer treatment. Nat. Rev. Drug Discov. *18*, 689–706. https://doi.org/10.1038/s41573-019-0029-0.

11. Guo, Z.S., Lu, B., Guo, Z., Giehl, E., Feist, M., Dai, E., Liu, W., Storkus, W.J., He, Y., Liu, Z., and Bartlett, D.L. (2019). Vaccinia virus-mediated cancer immunotherapy: cancer vaccines and oncolytics. J. Immunother. Cancer *7*, 6. https://doi.org/10.1186/s40425-018-0495-7.

12. Kirn, D.H., and Thorne, S.H. (2009). Targeted and armed oncolytic poxviruses: a novel multi-mechanistic therapeutic class for cancer. Nat. Rev. Cancer *9*, 64–71. https://doi.org/10.1038/nrc2545.

13. Hannigan, B.M., Barnett, Y.A., Armstrong, D.B.A., McKelvey-Martin, V.J., and McKenna, P.G. (1993). Thymidine kinases: the enzymes and their clinical usefulness. Cancer Biother. *8*, 189–197. https://doi.org/10.1089/cbr.1993.8.189.

14. Malfitano, A.M., Di Somma, S., Iannuzzi, C.A., Pentimalli, F., and Portella, G. (2020). Virotherapy: from single agents to combinatorial treatments. Biochem. Pharmacol. *177*, 113986. https://doi.org/10.1016/j.bcp.2020.113986.

15. Goncharova, E.P., Ruzhenkova, J.S., Petrov, I.S., Shchelkunov, S.N., and Zenkova, M.A. (2016). Oncolytic virus efficiency inhibited growth of tumour cells with multiple drug resistant phenotype in vivo and in vitro. J. Transl. Med. *14*, 241. https://doi.org/10.1186/s12967-016-1002-x.

16. Hofmann, E., Weibel, S., and Szalay, A.A. (2014). Combination treatment with oncolytic Vaccinia virus and cyclophosphamide results in synergistic antitumor effects in human lung adenocarcinoma bearing mice. J. Transl. Med. *12*, 197. https://doi.org/10.1186/1479-5876-12-197.

17. Liu, Z., Ravindranathan, R., Kalinski, P., Guo, Z.S., and Bartlett, D.L. (2017). Rational combination of oncolytic vaccinia virus and PD-L1 blockade works synergistically to enhance therapeutic efficacy. Nat. Commun. *8*, 14754. https://doi.org/10.1038/ncomms14754.

18. Heo, J., Breitbach, C.J., Moon, A., Kim, C.W., Patt, R., Kim, M.K., Lee, Y.K., Oh, S.Y., Woo, H.Y., Parato, K., et al. (2011). Sequential therapy with JX-594, a targeted oncolytic poxvirus, followed by sorafenib in hepatocellular carcinoma: preclinical and clinical demonstration of combination efficacy. Mol. Ther. *19*, 1170–1179. https://doi.org/10.1038/mt.2011.39.

19. Beljanski, V., and Hiscott, J. (2012). The use of oncolytic viruses to overcome lung cancer drug resistance. Curr. Opin. Virol. *2*, 629–635. https://doi.org/10.1016/j.coviro.2012.07.006.

20. Lun, X.Q., Jang, J.H., Tang, N., Deng, H., Head, R., Bell, J.C., Stojdl, D.F., Nutt, C.L., Senger, D.L., Forsyth, P.A., and McCart, J.A. (2009). Efficacy of systemically administered oncolytic vaccinia virotherapy for malignant gliomas is enhanced by combination therapy with rapamycin or cyclophosphamide. Clin. Cancer Res. *15*, 2777–2788. https://doi.org/10.1158/1078-0432.Ccr-08-2342.

21. Chen, W., Fan, W., Ru, G., Huang, F., Lu, X., Zhang, X., Mou, X., and Wang, S. (2018). Gemcitabine combined with an engineered oncolytic vaccinia virus exhibits a synergistic suppressive effect on the tumor growth of pancreatic cancer. Oncol. Rep. *41*, 67–76. https://doi.org/10.3892/or.2018.6817.

22. Ady, J.W., Heffner, J., Mojica, K., Johnsen, C., Belin, L.J., Love, D., Chen, C.T., Pugalenthi, A., Klein, E., Chen, N.G., et al. (2014). Oncolytic immunotherapy using recombinant vaccinia virus GLV-1h68 kills sorafenib-resistant hepatocellular carcinoma efficiently. Surgery *156*, 263–269. https://doi.org/10.1016/j.surg.2014.03.031.

23. Moehler, M., Heo, J., Lee, H.C., Tak, W.Y., Chao, Y., Paik, S.W., Yim, H.J., Byun, K.S., Baron, A., Ungerechts, G., et al. (2019). Vaccinia-based oncolytic immunotherapy Pexastimogene Devacirepvec in patients with advanced hepatocellular carcinoma after sorafenib failure: a randomized multicenter Phase IIb trial (TRAVERSE). Oncoimmunology *8*, 1615817. https://doi.org/10.1080/2162402x.2019.1615817.

24. Martins-Neves, S.R., Cleton-Jansen, A.M., and Gomes, C.M.F. (2018). Therapy-induced enrichment of cancer stem-like cells in solid human tumors: where do we stand? Pharmacol. Res. *137*, 193–204. https://doi.org/10.1016/j.phrs.2018.10.011.

25. Silva, I.A., Bai, S., McLean, K., Yang, K., Griffith, K., Thomas, D., Ginestier, C., Johnston, C., Kueck, A., Reynolds, R.K., et al. (2011). Aldehyde dehydrogenase in combination with CD133 defines angiogenic ovarian cancer stem cells that portend poor patient survival. Cancer Res. *71*, 3991–4001. https://doi.org/10.1158/0008-5472.CAN-10-3175.

26. Stacy, A.E., Jansson, P.J., and Richardson, D.R. (2013). Molecular pharmacology of ABCG2 and its role in chemoresistance. Mol. Pharmacol. *84*, 655–669. https://doi.org/10.1124/mol.113.088609.

27. Yoo, S.Y., Bang, S.Y., Jeong, S.N., Kang, D.H., and Heo, J. (2016). A cancer-favoring oncolytic vaccinia virus shows enhanced suppression of stem-cell like colon cancer. Oncotarget *7*, 16479–16489. https://doi.org/10.18632/oncotarget.7660.

28. Moreira, D., Silvestre, R., Cordeiro-da-Silva, A., Estaquier, J., Foretz, M., and Viollet, B. (2016). AMP-activated protein kinase as a target for pathogens: friends or foes? Curr. Drug Targets *17*, 942–953. https://doi.org/10.2174/1389450116666150416120559.

29. Xia, Y., Cheng, X., Li, Y., Valdez, K., Chen, W., and Liang, T.J. (2018). Hepatitis B virus deregulates the cell cycle to promote viral replication and a premalignant phenotype. J. Virol. *92*. e00722–18. https://doi.org/10.1128/JVI.00722-18.

30. Watanabe, T., Kawakami, E., Shoemaker, J.E., Lopes, T.J., Matsuoka, Y., Tomita, Y., Kozuka-Hata, H., Gorai, T., Kuwahara, T., Takeda, E., et al. (2014). Influenza virus-host interactome screen as a platform for antiviral drug development. Cell Host Microbe *16*, 795–805. https://doi.org/10.1016/j.chom.2014.11.002.

31. DeCotiis, J.L., and Lukac, D.M. (2017). KSHV and the role of notch receptor dysregulation in disease progression. Pathogens *6*, 34. https://doi.org/10.3390/pathogens6030034.

32. Seo, E.J., Kwon, Y.W., Jang, I.H., Kim, D.K., Lee, S.I., Choi, E.J., Kim, K.H., Suh, D.S., Lee, J.H., Choi, K.U., et al. (2016). Autotaxin regulates maintenance of ovarian cancer stem cells through lysophosphatidic acid-mediated autocrine mechanism. Stem Cells *34*, 551–564. https://doi.org/10.1002/stem.2279.

33. Bonjardim, C.A. (2017). Viral exploitation of the MEK/ERK pathway - a tale of vaccinia virus and other viruses. Virology *507*, 267–275. https://doi.org/10.1016/j.virol.2016.12.011.

34. Parato, K.A., Breitbach, C.J., Le Boeuf, F., Wang, J., Storbeck, C., Ilkow, C., Diallo, J.S., Falls, T., Burns, J., Garcia, V., et al. (2012). The oncolytic poxvirus JX-594 selectively replicates in and destroys cancer cells driven by genetic pathways commonly activated in cancers. Mol. Ther. *20*, 749–758. https://doi.org/10.1038/mt.2011.276.

35. Pant, A., Dsouza, L., Cao, S., Peng, C., and Yang, Z. (2021). Viral growth factor- and STAT3 signaling-dependent elevation of the TCA cycle intermediate levels during vaccinia virus infection. PLoS Pathog. *17*, e1009303. https://doi.org/10.1371/journal.ppat.1009303.

36. Han, J., Liu, Y., Yang, S., Wu, X., Li, H., and Wang, Q. (2021). MEK inhibitors for the treatment of non-small cell lung cancer. J. Hematol. Oncol. *14*, 1. https://doi.org/10.1186/s13045-020-01025-7.

37. Kanehisa, M., Furumichi, M., Sato, Y., Ishiguro-Watanabe, M., and Tanabe, M. (2021). KEGG: integrating viruses and cellular organisms. Nucleic Acids Res. *49*, D545–D551. https://doi.org/10.1093/nar/gkaa970.

38. Bommareddy, P.K., Aspromonte, S., Zloza, A., Rabkin, S.D., and Kaufman, H.L. (2018). MEK inhibition enhances oncolytic virus immunotherapy through increased tumor cell killing and T cell activation. Sci. Transl. Med. *10*, eaau0417. https://doi.org/10.1126/scitranslmed.aau0417.

39. Bagheri, N., Shiina, M., Lauffenburger, D.A., and Korn, W.M. (2011). A dynamical systems model for combinatorial cancer therapy enhances oncolytic adenovirus efficacy by MEK-inhibition. PLoS Comput. Biol. *7*, e1001085. https://doi.org/10.1371/journal.pcbi.1001085.

40. Roulstone, V., Pedersen, M., Kyula, J., Mansfield, D., Khan, A.A., McEntee, G., Wilkinson, M., Karapanagiotou, E., Coffey, M., Marais, R., et al. (2015). BRAF- and MEK-targeted small molecule inhibitors exert enhanced antimelanoma effects in combination with oncolytic reovirus through ER stress. Mol. Ther. *23*, 931–942. https://doi.org/10.1038/mt.2015.15.

41. Gholami, S., Chen, C.H., Gao, S., Lou, E., Fujisawa, S., Carson, J., Nnoli, J.E., Chou, T.C., Bromberg, J., and Fong, Y. (2014). Role of MAPK in oncolytic herpes viral therapy in triple-negative breast cancer. Cancer Gene Ther. *21*, 283–289. https://doi.org/10.1038/cgt.2014.28.

42. Botta, G., Passaro, C., Libertini, S., Abagnale, A., Barbato, S., Maione, A.S., Hallden, G., Beguinot, F., Formisano, P., and Portella, G. (2012). Inhibition of autophagy enhances the effects of E1A-defective oncolytic adenovirus dl922-947 against glioma cells in vitro and in vivo. Hum. Gene Ther. *23*, 623–634. https://doi.org/10.1089/hum.2011.120.

43. Gilmartin, A.G., Bleam, M.R., Groy, A., Moss, K.G., Minthorn, E.A., Kulkarni, S.G., Rominger, C.M., Erskine, S., Fisher, K.E., Yang, J., et al. (2011). GSK1120212 (JTP-74057) is an inhibitor of MEK activity and activation with favorable pharmacokinetic properties for sustained in vivo pathway inhibition. Clin. Cancer Res. *17*, 989–1000. https://doi.org/10.1158/1078-0432.Ccr-10-2200.

44. Subbiah, V., Kreitman, R.J., Wainberg, Z.A., Cho, J.Y., Schellens, J.H.M., Soria, J.C., Wen, P.Y., Zielinski, C., Cabanillas, M.E., Urbanowitz, G., et al. (2018). Dabrafenib and trametinib treatment in patients with locally advanced or metastatic BRAF V600-mutant anaplastic thyroid cancer. J. Clin. Oncol. *36*, 7–13. https://doi.org/10.1200/jco.2017.73.6785.

45. Hoffner, B., and Benchich, K. (2018). Trametinib: a targeted therapy in metastatic melanoma. J. Adv. Pract. Oncol. *9*, 741–745. https://doi.org/10.6004/jadpro.2018.9.7.5.

46. Kelly, R.J. (2018). Dabrafenib and trametinib for the treatment of non-small cell lung cancer. Expert Rev. Anticancer Ther. *18*, 1063–1068. https://doi.org/10.1080/14737140.2018.1521272.

47. Kato, S., McFall, T., Takahashi, K., Bamel, K., Ikeda, S., Eskander, R.N., Plaxe, S., Parker, B., Stites, E., and Kurzrock, R. (2021). KRAS-mutated, estrogen receptor-positive low-grade serous ovarian cancer: unraveling an exceptional response mystery. Oncologist *26*, e530–e536. https://doi.org/10.1002/onco.13702.

48. Chesnokov, M.S., Khan, I., Park, Y., Ezell, J., Mehta, G., Yousif, A., Hong, L.J., Buckanovich, R.J., Takahashi, A., and Chefetz, I. (2021). The MEK1/2 pathway as a therapeutic target in high-grade serous ovarian carcinoma. Cancers *13*, 1369. https://doi.org/10.3390/cancers13061369.

49. Bishnu, A., Phadte, P., Dhadve, A., Sakpal, A., Rekhi, B., and Ray, P. (2021). Molecular imaging of the kinetics of hyperactivated ERK1/2-mediated autophagy during acquirement of chemoresistance. Cell Death Dis. *12*, 161. https://doi.org/10.1038/s41419-021-03451-y.

50. Nagathihalli, N.S., Castellanos, J.A., Lamichhane, P., Messaggio, F., Shi, C., Dai, X., Rai, P., Chen, X., VanSaun, M.N., and Merchant, N.B. (2018). Inverse correlation of STAT3 and MEK signaling mediates resistance to RAS pathway inhibition in pancreatic cancer. Cancer Res. *78*, 6235–6246. https://doi.org/10.1158/0008-5472.CAN-18-0634.

51. Vultur, A., Villanueva, J., Krepler, C., Rajan, G., Chen, Q., Xiao, M., Li, L., Gimotty, P.A., Wilson, M., Hayden, J., et al. (2014). MEK inhibition affects STAT3 signaling and invasion in human melanoma cell lines. Oncogene *33*, 1850–1861. https://doi.org/10.1038/onc.2013.131.

52. Xie, B., Zhang, L., Hu, W., Fan, M., Jiang, N., Duan, Y., Jing, D., Xiao, W., Fragoso, R.C., Lam, K.S., et al. (2019). Dual blockage of STAT3 and ERK1/2 eliminates radioresistant GBM cells. Redox Biol. *24*, 101189. https://doi.org/10.1016/j.redox.2019.101189.

53. Kuchipudi, S.V. (2015). The complex role of STAT3 in viral infections. J. Immunol. Res. *2015*, 272359. https://doi.org/10.1155/2015/272359.

54. Okemoto, K., Wagner, B., Meisen, H., Haseley, A., Kaur, B., and Chiocca, E.A. (2013). STAT3 activation promotes oncolytic HSV1 replication in glioma cells. PLoS One *8*, e71932. https://doi.org/10.1371/journal.pone.0071932.

55. Peng, C., Zhou, Y., Cao, S., Pant, A., Campos Guerrero, M.L., McDonald, P., Roy, A., and Yang, Z. (2020). Identification of vaccinia virus inhibitors and cellular functions necessary for efficient viral replication by screening bioactives and FDA-approved drugs. Vaccines (Basel) *8*, 401. https://doi.org/10.3390/vaccines8030401.

56. Matveeva, O.V., and Chumakov, P.M. (2018). Defects in interferon pathways as potential biomarkers of sensitivity to oncolytic viruses. Rev. Med. Virol. *28*, e2008. https://doi.org/10.1002/rmv.2008.

57. Ying, L., Cheng, H., Xiong, X.W., Yuan, L., Peng, Z.H., Wen, Z.W., Ka, L.J., Xiao, X., Jing, C., Qian, T.Y., et al. (2017). Interferon alpha antagonizes the anti-hepatoma activity of the oncolytic virus M1 by stimulating anti-viral immunity. Oncotarget *8*, 24694–24705. https://doi.org/10.18632/oncotarget.15788.

58. Stewart, C.E., Randall, R.E., and Adamson, C.S. (2014). Inhibitors of the interferon response enhance virus replication in vitro. PLoS One *9*, e112014. https://doi.org/10.1371/journal.pone.0112014.

59. El-Jesr, M., Teir, M., and Maluquer de Motes, C. (2020). Vaccinia virus activation and antagonism of cytosolic DNA sensing. Front. Immunol. *11*, 568412. https://doi.org/10.3389/fimmu.2020.568412.

60. Islam, S.M.B.U., Hong, Y.M., Ornella, M.S.C., Ngabire, D., Jang, H., Cho, E., Kim, E.K., Hale, J.J.J., Kim, C.H., Ahn, S.C., et al. (2020). Engineering and preclinical evaluation of western reserve oncolytic vaccinia virus expressing A167Y mutant herpes simplex virus thymidine kinase. Biomedicines *8*, 426. https://doi.org/10.3390/biomedicines8100426.

61. Pourianfar, H.R., Javadi, A., and Grollo, L. (2012). A colorimetric-based accurate method for the determination of enterovirus 71 titer. Indian J. Virol. *23*, 303–310. https://doi.org/10.1007/s13337-012-0105-0.

62. Carbon, S., Ireland, A., Mungall, C.J., Shu, S., Marshall, B., Lewis, S., Ami, G.O.H., and Web Presence Working, G. (2009). AmiGO: online access to ontology and annotation data. Bioinformatics *25*, 288–289. https://doi.org/10.1093/bioinformatics/btn615.